

Ultra-Wideband Pulse-Based Directional Modulation

Himanshu Aggrawal
Department of Electrical
and Computer Engineering
Rice University
Houston, TX, USA

Rafael Puhl
Department of Electrical
and Computer Engineering
Rice University
Houston, TX, USA

Aydin Babakhani
Department of Electrical
and Computer Engineering
Rice University
Houston, TX, USA

Abstract—This paper presents a time-domain pulse-based directional modulation technique that enables secure wireless communication at the physical level. We use a train of sub-200psec pulses to achieve an information beamwidth of 1° while using antennas with a broad radiation pattern. The proposed technique leverages the advantages of a pulse-based system to demonstrate secure communication.

I. PULSE COMMUNICATION

Conventional wireless communication links consist of a transmitter and a receiver in which the directivity is predominantly defined by the radiation pattern of the antenna [1]. A problem of security in such conventional systems arises due to the wide pattern beamwidth of the transmitting antennas. Any sensitive receiver [2]–[4], even the ones outside the main lobe of the radiation, can receive and decode the information, making the system spatially insecure. Near Field Directional Modulation (NFDAM) systems [5], [6] modulate the signal at the antenna level to make the *information beamwidth* narrow and directional, without narrowing the radiation pattern. NFDAM (or directional modulation) transmitters scramble the signal constellation points outside the main information beamwidth, thus preventing even a sensitive receiver from decoding the signal outside the information beamwidth. Most of the prior literature on directional modulation has focused on narrow-band continuous-wave transmitters [5], [6].

In this paper, we introduce a broadband time-domain pulse-based directional antenna modulation architecture that can substantially increase the security of wireless communication. In the proposed architecture, multiple widely spaced transmitting antennas are tightly synchronized [7] at the symbol level to generate a very narrow ($\sim 1^\circ$) information beamwidth.

A. Proposed Idea

A *spatial encoding* architecture is presented in which we synchronize multiple widely spaced transmitting antennas at the symbol level to generate information that is focused to a small spatial location. This information cannot be decoded from a reflected path, nor from in front of or behind the intended target location. The reported technique shapes pulses across antennas with different portions of the information encoded on different antennas. This contrasts with conventional wireless communication systems, in which the complete constellation symbol is transmitted from one antenna, or, in the case of highly directional phased arrays, from all antennas via a phase offset per antenna. Spatial encoding fundamentally differs in the topology: instead of sending the

complete constellation symbol (complete information) from a single antenna, a part of the symbol (semi-symbol), which is a fraction of the total amplitude, is sent from one antenna and the remaining fraction is sent from other antennas. The transmitting antennas are tightly synchronized at the symbol level. A receiver that is placed exactly at the focus point, where all the semi-symbols arrive at the same time, sees the correct complete symbol. The point where all the semi-symbols combine coherently is unique in space; this being so, the communication can be said to be spatially encoded or spatially encrypted.

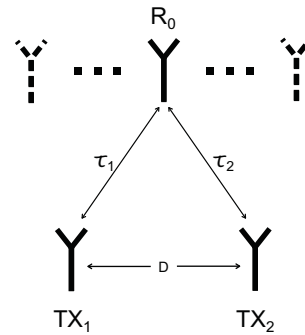


Fig. 1. Information generation with two tightly synchronized transmitters

We illustrate spatial encoding via an example with two transmitting elements, as shown in Fig.1. Let $S_{\text{orig}}(t)$ be the signal that corresponds to a complete symbol. This signal is divided into two overlapping semi-symbols, $S_1(t)$ and $S_2(t)$, such that $S_{\text{orig}}(t) = S_1(t) + S_2(t)$. These two signals $S_1(t)$ and $S_2(t)$ are generated at Tx_1 and Tx_2 , respectively, using two synchronized base-band waveform generators. Assuming there is a separation of D between Tx_1 and Tx_2 , the signal received at different angles in space will be $S_1(t-\tau_1) + S_2(t-\tau_2)$, where τ_1 and τ_2 are the propagation delays from Tx_1 and Tx_2 to a point P in space, respectively. As shown in Fig.1, if point P is located equidistantly from Tx_1 and Tx_2 , both signals will reach at the same time and will overlap/coincide with each other, thus generating the desired signal/symbol. However, if $\tau_1 \neq \tau_2$, the received signal will be $S_1(t-\tau_1) + S_2(t-\tau_2)$ which is distorted and non-overlapping.

B. Working Explained

For the sake of simplicity and without losing any generality, two transmitters (Tx_1 and Tx_2) and one receiver (Rx) are chosen. The two transmitters are synchronized time-domain

Tx1 (Semi-symbol)	0.1	0.1	0.2	0.1	0.2	0.3	0.1	0.2	0.3	0.4	0.2	0.3	0.4
Tx2 (Semi-symbol)	0.1	0.2	0.1	0.3	0.2	0.1	0.4	0.3	0.2	0.1	0.4	0.3	0.2
Tx1+Tx2 (Complete symbol) [Bits]	0.2	0.3 [00]		0.4 [01]			0.5 [10]				0.6 [11]		

TABLE I. SYMBOL GENERATION AT A DESIRED ANGLE WITH TWO ANTENNAS

short-pulse generators with amplitude modulation capability. The transmitters have 10 steps of amplitude modulation (e.g. 0.1, 0.2 ... 0.9, 1.0). For simplicity, only the first 2 bits (four levels) of modulation are used (from 0.1–0.4). Thus, each transmitter can transmit 2 bits of amplitude-modulated synchronized Gaussian pulses (semi-symbols). The received signal for an equidistant receiver will be the sum of the transmitted signals (semi-symbols), in which the amplitude corresponds to a certain bit value.

From here on, bit values are assigned to corresponding received amplitudes. For instance, a received signal with peak-to-peak voltage of 0.3V will be referred to as bit “00,” 0.4V as bit “01,” and so on, as shown in Table I.

For instance, if Tx₁ transmits semi-symbol X₁ and Tx₂ transmits semi-symbol X₂, the received signal will be the sum of the transmitted signals, X₁+X₂. For two different transmitted semi-symbols, the received symbol will be the same as long as their sum is constant and the receiver is equidistant from both the transmitters. However, in the case when the receiver is not equidistant, there will be no or partial overlapping of the semi-symbols, which will distort the received symbol. This distorted symbol will have a different peak-to-peak amplitude than the sum of the two semi-symbols. This incorrect amplitude will correspond to a different bit and thus will be read erroneously by an eavesdropper. Moreover, with the possibility of assigning different semi-symbols for the same transmitted symbol, the statistical symbol recovery for an eavesdropper becomes even more difficult. This may be further understood from Fig.2.

Table 1 tabulates all the possible combinations of transmitted and received symbols for an equidistant receiver antenna.

1) *Division algorithm*: The semi-symbols for each transmitter are generated based on the final symbol to be sent. For instance, if bit “10” is to be sent, the transmitters randomly chooses one of the four possible semi-symbol combinations, as shown in Table I.

2) *Receiver decoding algorithm*: The receiver is in the line of sight (LOS) of the transmitters. It uses the amplitude of the combined signals to detect different symbols. A look-up table is used to convert the detected amplitude to bits. The generation of this table is discussed on the next page

3) *Beam steering/focusing capability*: It is important to note that even though the results are discussed for an equidistant receiver, the desired focus point of the system can be changed by introducing proper relative delays in the transmitters. These delays will determine the point in space where the semi-symbol combines correctly, providing the lowest Bit Error Rate (BER) during communication. Thus, one of the advantages of this topology is the convenience of changing the direction of the information beam by introducing relative delays in the transmitters. Consequently, the receiver can be securely localized, not only in angle but also in distance,

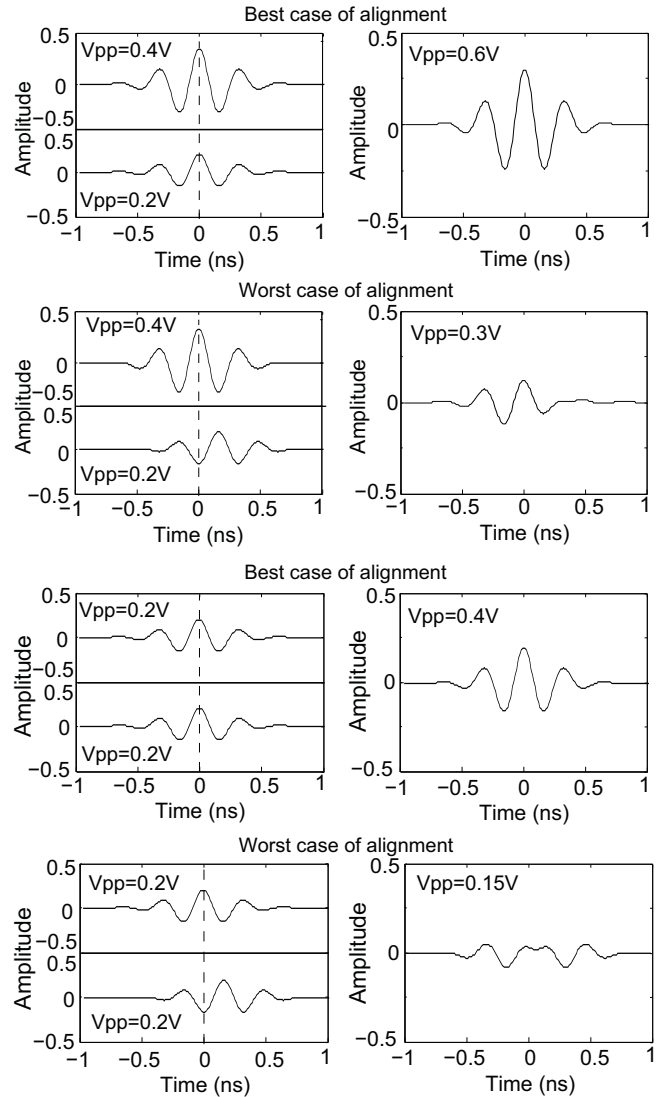


Fig. 2. Pulse combining in air

as a key property of the spatial encoding’s ability to focus information.

C. Experimental Setup

The experimental setup consists of an arbitrary waveform generator, which generates two streams of synchronized pulses. These pulses are amplified and transmitted using impulse antennas designed to operate in the 3–10 GHz band. A similar impulse antenna is used as a receiver. The received signal is amplified by a LNA before being sampled by a 25GS/s real-time oscilloscope. The two transmitters are placed at a distance of 0.6m, and the receiver antenna is placed at a distance of 1.2m from a line connecting the two transmitters, as shown

in Fig.3. The cable length is carefully calibrated so that the pulses reach the transmitting antennas at the same time. The whole setup is automated using a Matlab code. In this setup, a master computer communicates with the instruments using the GPIB-VISA protocol.

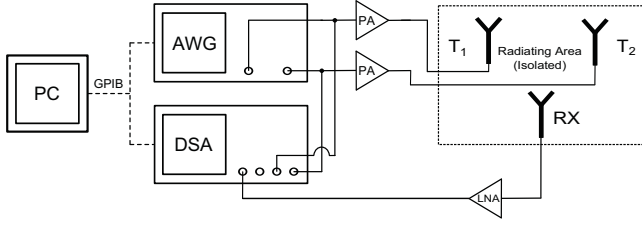


Fig. 3. Experimental setup to demonstrate spatial encoding

D. Setup Calibration and Table Generation

It is important to calibrate the system before performing the Bit Error (BER) test. The system is calibrated by each transmitter sending all possible bits. Based on the received signal, the gain of the amplifier is recorded. The non-linearity in the gain of the amplifier is compensated for by predistorting the input signal.

A look-up table is generated by sending random bits and recording the maximum and minimum voltage levels for each symbol. For instance, the symbol corresponding to bit “00” (0.3 volts) is transmitted with all possible semi-symbol combinations. Even after performing the predistortion, for a desired symbol value of 0.3V, the receiver may receive a value between 0.28V to 0.31V, which is due to the nonlinearity in the system. This level of error in the proposed architecture can be tolerated. Finally, the thresholds are set midway between the symbol voltages, and corresponding bits are assigned, as shown in Fig.4.

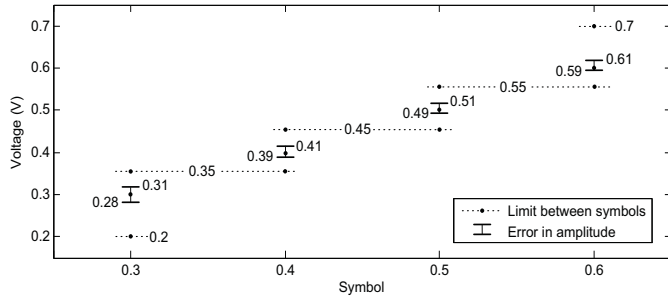


Fig. 4. Setting threshold midway between the symbol voltages

E. Results

To measure BER, a pseudo-random number generator is used to generate the transmitted bits. These bits are decomposed into symbols; the symbols are then broken down into multiple pairs of semi-symbols. All these pairs of semi-symbols will generate the same complete symbol at the desired direction of transmission. A random generator picks one of these pairs and assigns it to two transmitting antennas. This random selection of a semi-symbol pair increases the complexity for an eavesdropper to perform a statistical

recovery. The received signal is then compared against the look-up table introduced earlier. Finally, the BER is calculated by comparing the received bits with the transmitted bits.

1) *Time Domain Radiation Pattern of One Versus Two Antennas:* The radiation pattern of a single-impulse antenna is derived by measuring the power of the radiated pulse as a function of angle, as shown in the Fig.5. As expected, the radiation pattern of the single antenna is very broad. Shown with dots is the power of the received pulse from two separate synchronized transmitting antennas. At the center, both the pulses overlap constructively, resulting in higher amplitude. However, as the receiver moves away from the center, two pulses arrive at different times. The received pulse amplitude reaches a minima when the maxima of one transmitted pulse overlaps with the minima of another. This first occurs when the differential delay between the pulses is half the pulse width. Thus, by changing the pulse width, it is possible to change the location of the first null point.

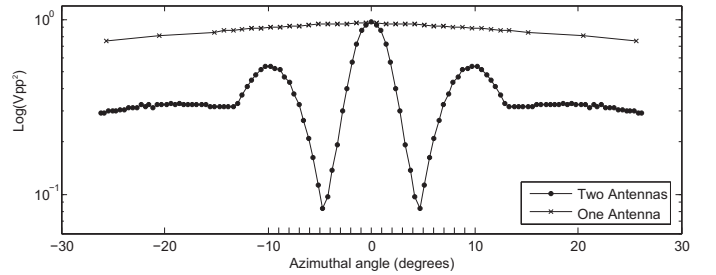


Fig. 5. Effective radiation pattern

2) *Symbol Collapsing:* As the receiver moves away from the center, one of the transmitted signals adds more delay. This differential delay causes partial symbol overlap. This partial overlap, combined with the possibility of sending multiple semi-symbols for the same complete symbol results in a range of received amplitudes that overlaps with the amplitude of the other symbols (Fig.2). This phenomenon results in higher BER for the receivers that are not located at the desired angle. The angular range between the two null points in Fig.5 creates a void zone, near and beyond which the symbols cannot be distinguished, so the communication link cannot be established. Moreover, by reducing the pulse width, the void zone becomes smaller, resulting in a smaller information beamwidth.

3) *Radiation Pattern Versus Information Pattern:* An information pattern is used to represent the spatial information distribution of a communication system. Fig.6 shows the BER of two synchronized pulse-transmitting antennas.

In this experiment, a BER of 10^{-2} at 1° and 10^{-6} at 0.47° was recorded. A linear extrapolation of these results gives a BER of less than 10^{-10} at the center.

An important observation to make is that the BER increases rapidly as the receiver moves away from the center. This phenomenon is caused due to the symbol collapsing. In addition to this, the reduction in pulse width brings the null points in Fig.5 closer to the center, and symbol collapsing happens at a smaller angle. This effect enhances the security of the wireless link by making the BER well even sharper.

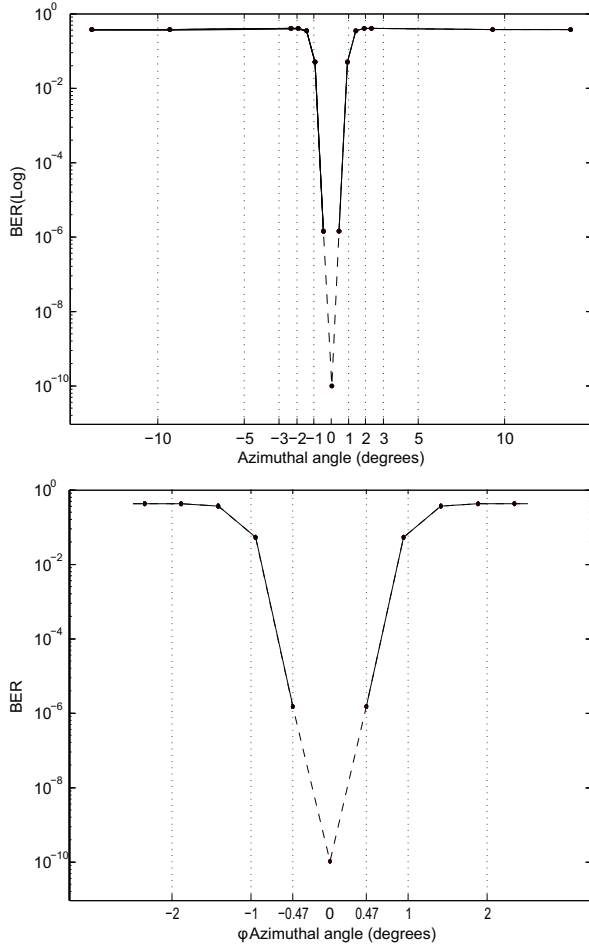


Fig. 6. Measured Bit Error Rate (BER) of the system. Top figure is the measurement across wide range of Azimuthal angle, bottom figure is the zoomed version between $0-2^\circ$ (The BER measurement has been done for left side and mirrored right side, leveraging symmetry in the system)

II. ADVANTAGES OF PULSE-BASED SYSTEMS OVER CONTINUOUS WAVE SYSTEMS

One of the major advantages of pulse-based systems over conventional continuous wave systems is their ability to mitigate a multi-path effect [8], [9]. In the case of pulse-based systems, the multi-path reflections will arrive at a different time; later than the one directly reflected from the object. Thus, it is easier to eliminate such multi-path reflected signals in time-domain based systems by discarding the signal that comes at a later time. In the case of continuous wave systems, however, the multi-path reflected signals interact with the line-of-sight reflected signal and changes the phase of the received signal.

The proposed pulse-based communication system adds an extra level of security at the symbol level. This makes it extremely difficult for an eavesdropper outside the information beamwidth to decode the transmitted symbols. Such secure communication schemes are extremely useful in point-to-point, directional, high data-rate transmission links [10]. This scheme can be of significant importance in base-station to base-station links or in establishing secure communication between two military bases.

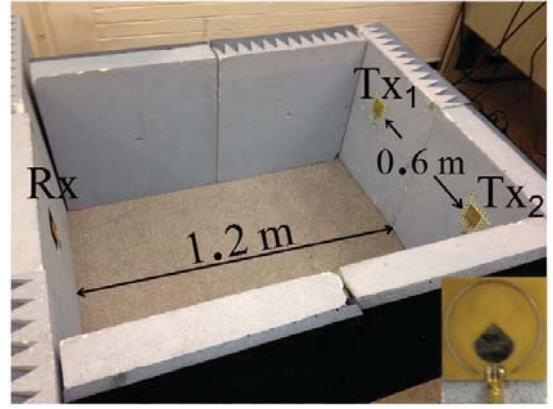


Fig. 7. Experimental setup to demonstrate spatial encoding

III. CONCLUSION

In this paper, an ultra-wideband pulse-based directional modulation technique is presented for secure communication. The introduced spatial encoding provides a key building block for preventing eavesdroppers as the complete symbol is not present at unintended locations. Finally, an information beamwidth of 1° is achieved using antennas with a broad radiation pattern and sub-200ps pulses.

IV. ACKNOWLEDGMENT

The authors acknowledge the help of Mahdi Assefzadeh in the design of the impulse antennas.

REFERENCES

- [1] G. Shiroma, R. Miyamoto, J. Roque, J. Cardenas, and W. Shiroma, "A High-Directivity Combined Self-Beam/Null-Steering Array for Secure Point-to-Point Communications," *IEEE Transactions on Microwave Theory and Techniques*, May 2007.
- [2] C.-M. Lai, J.-M. Wu, P.-C. Huang, and T.-S. Chu, "A scalable direct-sampling broadband radar receiver supporting simultaneous digital multibeam array in 65nm CMOS," in *IEEE International Solid-State Circuits Conference Digest of Technical Papers (ISSCC)*, Feb 2013.
- [3] C. Keller, J. Burkhart, and T. Phuong, "Ultra-Wideband Direct Sampling Receiver," in *IEEE International Conference on Ultra-Wideband*, Sept 2007.
- [4] H. Aggrawal and A. Babakhani, "A 40GS/s Track-and-Hold amplifier with 62dB SFDR3 in 45nm CMOS SOI," in *IEEE MTT-S International Microwave Symposium (IMS)*, 2014.
- [5] A. Babakhani, D. Rutledge, and A. Hajimiri, "Transmitter Architectures Based on Near-Field Direct Antenna Modulation," *IEEE Journal of Solid-State Circuits*, Dec 2008.
- [6] A. Babakhani, D. B. Rutledge, and A. Hajimiri, "Near-field direct antenna modulation," *IEEE Microwave Magazine*, vol. 10, no. 1, pp. 36-46, 2009.
- [7] H. Aggrawal and A. Babakhani, "An Ultra-Wideband Impulse Receiver for sub-100fsec Time-Transfer and sub-30m Localization," in *IEEE Radio and Wireless Symposium*, 2016.
- [8] M. DongLin, L. Fansheng, and S. Jie, "Simulation on Multi-path Fading in Wireless Channel," in *International Conference on Computer Science and Electronics Engineering*, 2012.
- [9] X. Duan, H. Liu, J. Li, and Z. He, "CLEAN algorithm based direct-path-interference and multi-path-interference suppression in Bistatic MIMO Radar," in *International Workshop on Microwave and Millimeter Wave Circuits and System Technology*, 2012.
- [10] M.-C. Chang, "Terahertz CMOS circuit design and applications for ultra-high data rate ($>100\text{Gbps}$) communication," in *IEEE 8th International Conference on ASIC*, 2009.